

## Using wavelet de-noised spectra in NMR screening

Nikola Trbovic<sup>a,1</sup>, Felician Dancea<sup>a,1</sup>, Thomas Langer<sup>b</sup>, Ulrich Günther<sup>c,\*</sup>

<sup>a</sup> Center for Biomolecular Magnetic Resonance (BMRZ), Institute of Biophysical Chemistry, J.W. Goethe University, Marie-Curie-Str. 9, 60439 Frankfurt, Germany

<sup>b</sup> Center for Biomolecular Magnetic Resonance (BMRZ), Institute of Organic Chemistry and Chemical Biology, J.W. Goethe University, Marie-Curie-Str. 11, 60439 Frankfurt, Germany

<sup>c</sup> CR UK Institute for Cancer Studies, University of Birmingham, HWB-NMR, Vincent Drive, Edgbaston, Birmingham B15 2TT, UK

Received 5 April 2004; revised 19 November 2004

Available online 28 January 2005

### Abstract

Principal component analysis (PCA) is a commonly used algorithm in multivariate analysis of NMR screening data. PCA substantially reduces the complexity of data in which a large number of variables are interrelated. For series of NMR spectra obtained for ligand binding, it is commonly used to visually group spectra with a similar response to ligand binding. A series of filters are applied to the experimental data to obtain suitable descriptors for PCA which optimize computational efficiency and minimize the weight of small chemical shift variations. The most common filter is bucketing where adjacent points are summed to a bucket. To overcome some inherent disadvantages of the bucketing procedure we have explored the effect of wavelet de-noising on multivariate analysis, using a series of HSQC spectra of proteins with different ligands present. The combination of wavelet de-noising and PCA is most efficient when PCA is applied to wavelet coefficients. This new algorithm yields good clustering and can be applied to series of one- or two-dimensional spectra.

© 2005 Elsevier Inc. All rights reserved.

**Keywords:** NMR screening; PCA; Wavelet transform

### 1. Introduction

NMR spectroscopy has become an important technique in screening for protein inhibitors. Both, NMR spectra of isotopically labeled proteins or the spectra of the inhibitors can be used for ligand screening [1,2]. When protein spectra are employed to detect ligand binding the enormous sensitivity of the <sup>1</sup>H and <sup>15</sup>N chemical shifts of the protein backbone for small geometric or electrostatic changes induced by ligand binding is exploited. For ligand based screening a great variety of NMR methods including transferred NOEs [3,4], saturation transfer difference (STD) experiments [5–7], ePHOGSY [8], diffusion editing [9] or NOE pump-

ing [10,11] are used. Most of these techniques can be utilized for rational drug design studying the effect of specific changes in inhibitors as well as for screening of large numbers of inhibitors. NMR also starts to play a significant role in applications where biological samples such as bio-fluids or tissue extracts are the subject of investigations [12]. In fact, NMR screening using predominantly one-dimensional spectra of body fluids has become an important technique in metabonomics to study toxicity and gene function [13]. Similarly, NMR has been used to screen fruit juices [14,15] or beer [16] as a measure of quality control.

To analyze large numbers of spectra for changes and similarities efficient pattern recognition methods such as principal component analysis (PCA) are commonly used. Principal components are linear combinations of the original data which help to visualize similarities in an ensemble of spectra. Since all principal components

\* Corresponding author. Fax: +44 121 414 8357.

E-mail address: [u.l.gunther@bham.ac.uk](mailto:u.l.gunther@bham.ac.uk) (U. Günther).

<sup>1</sup> These authors made equal contributions to this work.

are orthogonal and ordered with respect to maximum variance between the samples, the largest two or three principal components provide an excellent representation of variability within a set of data. Spectra with little variance compared to the reference spectrum will form a group around the reference. Outliers usually represent hits in ligand screening. Unfortunately PCA is computationally expensive, even if only few principal components are calculated. Several data manipulations are usually applied prior to PCA, mainly to reduce the data size, but also to minimize artifacts. Simple thresholding helps to eliminate noise-related alterations between the spectra. In addition, in a procedure called ‘bucketing’ [17], adjacent data points (in the case of two-dimensional spectra a rectangular subsection of the spectrum) are added to one ‘bucket’ thus reducing the amount of data points. This procedure is broadly used in common NMR screening software. Bucketing helps to eliminate artifacts by averaging small chemical shift perturbations arising from small variations in pH or other sample conditions and reduces the size of the data. The ‘bucket’ descriptors which are subsequently used in PCA maintain much of the information of the spectrum although details which are only available at high resolution may be lost. Bucketing is also prone to introduce artifacts when peaks experience small chemical shift perturbations at the border between buckets. In this case a large change may be detected for a small effect. Although unlikely, another artifact may arise from cancellations in the bucket when different points which contribute to one bucket add and subtract equal or similar intensities. In this case no or only a small overall effect is left in the bucket.

With higher resolution offered by increasing field strengths of NMR spectrometers PCA should preserve the full information available in the spectra. Here we demonstrate that a combination of PCA analysis with wavelet de-noising yields improved clustering with reduced artifacts. Application of PCA in wavelet space after thresholding preserves the resolution in the original data, is insensitive to small chemical shift changes and does not show the artifacts which are common to bucketing schemes.

## 2. Theoretical background

### 2.1. Principal component analysis

Principal component analysis is a linear transformation which can be used to visualize similarities and differences in large data sets. If  $X$  is a data matrix which contains  $m$  NMR spectra in columns with  $n$  frequencies in rows, we can estimate a reference centered covariance matrix of  $X$  as  $C_X = (X - X_r) \cdot (X - X_r)^T$ , where  $X_r$  is the reference data matrix which represents a reference spec-

trum. In the examples shown here the HSQC spectrum of the protein without ligand was used as a reference.

For fully uncorrelated NMR spectra, all off-diagonal elements of the  $C_X$  matrix are zero and the diagonal elements represent the variances of the individual rows. For correlated data the off-diagonal elements are the covariances between the different spectra. Noisy data represent a high-dimensionality problem because noisy NMR spectra are never fully correlated.

To reduce the dimensionality of a series of NMR spectra contained in the matrix  $X$  we try to find a linear transformation  $Y = M \cdot X$  to a new set of variables which have a diagonal covariance matrix  $C_Y$  (so that each of its elements is uncorrelated). The covariance matrices of  $X$  and  $Y$  are related by

$$C_X = M^T \cdot C_Y \cdot M. \quad (1)$$

Because  $C_Y$  is a diagonal and  $M$  is an orthonormal matrix, the columns of  $M^T$  are the eigenvectors of  $C_X$  while the diagonal elements of  $C_Y$  are the corresponding eigenvalues. If there are linear combinations among the elements of the original data matrix  $X$  then some of the eigenvalues in  $C_Y$  will vanish. For highly similar but not identical data sets the values of the eigenvalues in  $C_Y$  will be small. For the screening data used in this work these small eigenvalues represent spectra which are similar to the reference. PCA uses the covariance matrix of a set of experiments to find a transformation to a new set of uncorrelated variables. PCA starts with the covariance matrix of all the original data and ranks the principal components with respect to similarity to the reference. The most common algorithm used to calculate principal components is the singular value decomposition which solves the eigen decomposition problem in Eq. (1). For computational efficiency it is important that only the largest eigenvalues are calculated.

### 2.2. Discrete wavelet transform

Several recent publications showed the potential of wavelet based de-noising for NMR spectroscopy [18–21]. The principles of wavelet transforms and noise suppression employing wavelet transforms were described in detail in several excellent monographs [22,23]. Donoho and Johnstone [24,25] showed that suppression of wavelet coefficients has desirable statistical properties in the suppression of noise.

The discrete wavelet transform (DWT) decomposes a signal using a set of base functions  $\Psi_{jk}$  which are derived from a single mother wavelet  $\Psi$  by dyadic dilatations ( $j$ ) and translations about ( $k$ )

$$\Psi_{jk}(x) = 2^{j/2} \Psi(2^j x - k). \quad (2)$$

These wavelets are shifted by  $k$  and scaled by  $j$  and have compact support, i.e., the wavelet is zero outside the finite interval  $[k2^{-j}, (k+1)2^{-j}]$ . The wavelets  $\Psi_{jk}$  form an

orthonormal basis of  $L_2$ , the space of square integrable functions. For this reason any function  $S(x) \in L_2$  can be represented by the base functions  $\Psi_{jk}$  and corresponding scaling functions  $\Phi_{jk}$  ( $\Phi$  = father wavelet)

$$S(x) = \sum_k \alpha_k \Phi_{0k}(x) + \sum_j \sum_k \beta_{jk} \Psi_{jk}(x), \quad (3)$$

where the coefficients are

$$\alpha_k = \int S(x) \Phi_{0k}^*(x) dx, \quad \beta_{jk} = \int S(x) \Psi_{jk}^*(x) dx.$$

For a vector of function values  $S = \{S(x_1), S(x_2), \dots, S(x_N)\}'$  the discrete wavelet transform can be represented in matrix form as

$$w = \mathbf{W}S, \quad (4)$$

where  $\mathbf{W}$  is an  $N \times N$  orthogonal matrix associated with the chosen orthonormal wavelet basis and  $w$  is a  $N \times 1$  vector comprising both, wavelet coefficients and scaling coefficients. Since the wavelet is scaled and shifted the WT yields a time-frequency representation of the signal.

Several wavelets were designed to fulfill the basic requirements to have a compact support and to form an orthonormal system. The most basic wavelet is the Haar wavelet, a simple step function. More commonly used wavelets are Daubechies wavelets, Coiflets and Symmlets. In this work we used Symmlets with eight vanishing moments.

### 2.3. Wavelet de-noising

The basis of wavelet de-nosing is the property of wavelets to represent smooth signals with a sparse set of coefficients. Therefore, suppression of small coefficients can be used to de-noise signals. Many different algorithms to determine noise-related wavelet coefficients have been proposed. Global hard- or soft-thresholding are the most widely used methods [24,25]. In hard-thresholding all coefficients below a threshold  $\lambda$  are zeroed, while in the soft-thresholding besides zeroing all the other coefficients are shrunk towards zero by subtracting  $\lambda$ . In the present work we used soft-thresholding which provides good results on  $^{15}\text{N}$ -edited HSQC spectra. The threshold  $\lambda$  was determined using 'universal thresholding' [25] with a value of  $\lambda = \sigma\sqrt{2 \log N}$ , where  $\sigma$  represents the noise variance estimated on the highest decomposition level and  $N$  the total number of data points. The overall process of de-noising consists of a wavelet transform followed by thresholding and an inverse wavelet transform.

In addition to wavelet thresholding which has a smoothing effect on the spectra and suppresses noise it is also possible to apply a multiresolution analysis (MRA) [26]. It is based on the idea that a function or a signal can be approximated at different dilatation levels. This concept has previously been exploited for solvent suppression in NMR spectra in [27]. In a MRA

only a subset of the resolution levels can be used to restore the signal. This may be useful to suppress low or high frequency signal components represented at low or high dyadic levels. In this work both, soft-threshold de-noising and the suppression of coefficients at the lowest resolution levels were used to obtain determinants for the subsequent PCA.

### 3. Materials and methods

The data used in this study consisted of 101  $^{15}\text{N}$ ,  $^1\text{H}$ -HSQC spectra of the hsp90 protein in the presence of different ligands recorded on a BRUKER DMX 600 spectrometer. 1024 complex points were recorded in the direct dimension and 128 increments were recorded for each spectrum. All spectra were processed using NMRLab [28] with a quadratic sine apodization prior to the fast Fourier transform in both dimensions and automated two-dimensional phase correction (Günther, Ludwig unpublished). After stripping lines without signals from the spectra a data matrix of  $512 \times 512 \times 101$  real points was recovered for subsequent PCA analysis.

The 101 HSQC spectra were scaled using the mean of the largest signals with minimum variability within the data set. Subsequently different protocols were employed for the three analysis schemes shown in Fig. 1. For *scheme A* a threshold value of 20% of the largest point in each spectrum was applied prior to adding data points in  $16 \times 16$  point bucket cells. Subsequently common baseline regions of all spectra with zero intensity after thresholding were removed and the two-dimensional HSQC spectra were concatenated into one-dimensional objects prior to PCA analysis. In *scheme B* a wavelet de-nosing step was added before thresholding and bucketing using a one-dimensional discrete wavelet transform in both dimensions. The overall process of wavelet de-noising consists of four stages: (I) data scaling with respect to the average noise level estimated by the median absolute deviation of the wavelet coefficients on the first dyadic level ( $\sigma$ , see Section 2), (II) a discrete wavelet transform using a Symmlet (8) quadrature mirror filter and a low-frequency cutoff of 4, (III) a global soft-thresholding of the wavelet coefficients applying the universal threshold  $\lambda = \sqrt{2 \log N}$  (where  $N$  is the total number of data points) and (IV) an inverse discrete wavelet transform which returns a matrix with the same size as the input data matrix. The subsequent steps (thresholding, bucketing, concatenation, removal of common zeroes, and PCA) were identical with scheme A. In *scheme C* the scaled data were subject to a wavelet transform and soft-thresholding with identical parameters as in scheme B. Additional MRA was applied by suppressing four low-frequency dyadic levels. Data points zeroed in all spectra were eliminated after wavelet thresholding followed by concatenation.

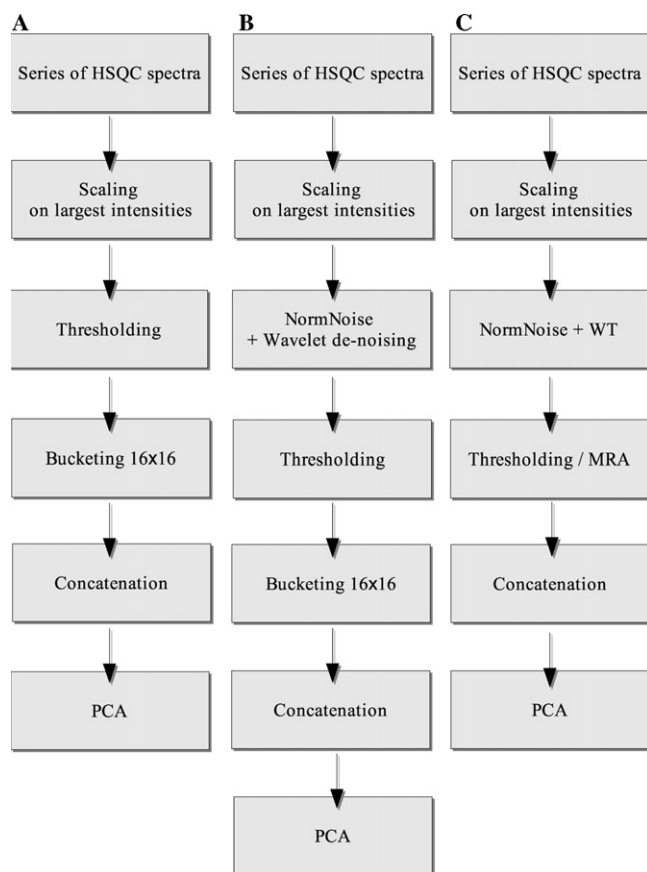


Fig. 1. Schematic representation of different PCA data reduction schemes: (A) bucketing scheme, (B) bucketing on de-noised data, and (C) PCA on wavelet coefficients.

Automated analysis of the PCA clusters was used to evaluate the PCA result. The clustering algorithm was based on the hierarchical clustering analysis [29], where objects are linked together based on the network of Euclidean distances between pairs of objects. In a first step binary clusters of objects in close proximity were formed. As objects were paired into binary clusters, the newly formed clusters were grouped into larger clusters until a hierarchical tree was formed. Finally, the hierarchical tree was divided into clusters of objects by detecting the natural groupings in the cluster tree. To allow the formation of a main cluster surrounded by several outliers, a tight clustering threshold was used to cut the hierarchical tree. The principal components were scaled with respect to the largest distance in the data set and a *clustering factor* was estimated as the mean scaled distance between the PCA outliers and the closest neighbor belonging to the main cluster. *Compression factors* were calculated as the ratio between the number of elements of the original data matrix and the number of elements of the pre-processed matrix used for the subsequent PCA. The *de-noising factor* describes the relative number of points eliminated by thresholding. In schemes A/B it is calculated as the quotient of the number of ele-

ments of the data matrix zeroed by thresholding and the total number of elements of the original matrix. For scheme C the quotient of the number of wavelet coefficients eliminated by thresholding and the total number of elements of the original matrix was used.

All routines were programmed in the MATLAB (The Mathworks) programming environment. The wavelet de-noising routines were based on the WAVELAB802 wavelet toolbox for MATLAB [18].

#### 4. Results

Here we show how wavelet de-noising and MRA analysis can be efficiently combined with PCA to analyze large series of NMR data. To demonstrate the advantage of a wavelet filter compared to the commonly used bucketing approach we examined different pre-processing schemes to reduce artifacts and the data size prior to PCA analysis. As a test data set we used 101 HSQC spectra of hsp90 with different ligands added. Data processing included a quadratic sine apodization prior to the fast Fourier transformation in both dimensions, scaling, thresholding, and concatenation of two-dimensional data matrices to data vectors (see Section 3).

Fig. 1 shows the three different PCA schemes which were compared. In scheme A a standard bucketing approach with  $16 \times 16$  buckets was used to reduce the size of the data. The result of this bucketing procedure is presented in the first panel of Fig. 2 which shows a plot of the first three principal components (pc1, pc2, and pc3). A cluster between 0 and 100 on pc1 and pc2 and  $-40$  and  $40$  on pc3 (blue '+') represents spectra with little change compared to the reference. Positive hits in the screening appear with negative values in pc2 (green '+'). In addition, spectra 42 and 28 (red '+') appear with large values in pc3. The corresponding spectra for both cases show few effects compared to the reference. Fig. 2D shows the HSQC spectrum of the complex form (protein with ligand, blue) superimposed on the reference spectrum (without ligand, red) for the false hit 42. In contrast, Fig. 2E shows an example for a positive hit with various small chemical shift changes compared to the reference.

In scheme B (Fig. 1) a wavelet de-noising step was applied prior to thresholding and bucketing (see Section 3 for details of the procedure). Here wavelet shrinkage is used for de-noising and smoothing of the spectra but not for data compression. Combined de-noising/bucketing depicted in Fig. 2B exhibits improved clustering in spectra of protein with non-binding ligands. In addition, some hits are clearly separated (green '+'). Spectrum 42 appears again as a false hit (red '+') whereas spectrum 28 joins the cluster around the reference. The improvement for spectrum 28 can be explained by the smoothing effect of wavelet thresholding on the spectrum.

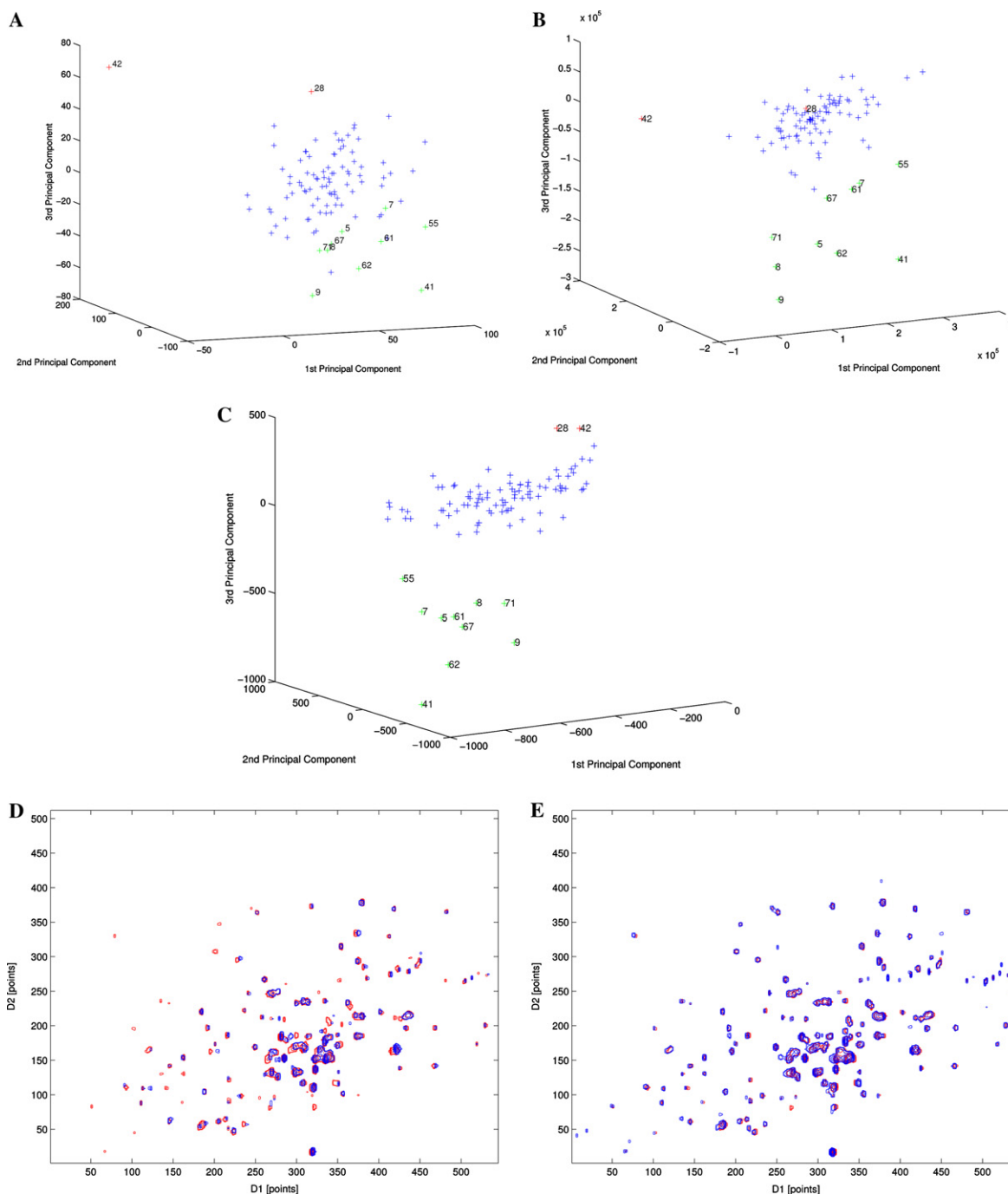


Fig. 2. (A) The first three principal component obtained using scheme A with  $16 \times 16$  bucketing prior to PCA for a set of 101 HSQC spectra of hsp90 recorded with different ligands. Each '+' represents one HSQC spectrum. (B) Principal components obtained using scheme B with  $16 \times 16$  bucketing on wavelet de-noised data using a Symmlet(8) quadrature mirror filter and soft-threshold de-noising prior to PCA. (C) Principal components obtained employing scheme C using a wavelet transform with a Symmlet(8) quadrature mirror filter prior to PCA. (D) Spectrum 41 (blue) superimposed to the reference spectrum (red, without ligand) showing significant chemical shift changes. (E) Spectrum 42 (blue) superimposed to the reference spectrum (red, without ligand) showing few chemical shift changes. (For interpretation of the references to color in this figure legend, the reader is referred to the web version of this paper.)

In scheme C (Fig. 1), PCA was applied directly to the wavelet coefficients. Since the wavelet transform is a unitary transformation (Eq. (4)), eigenvalues of the wavelet coefficients will be equivalent to the eigenvalues of the original data. Therefore, a PCA analysis performed di-

rectly on the wavelet coefficients conveys the multivariate properties as if it was applied to the original data. The wavelet coefficient thresholding has a triple effect: it eliminates the stochastic component of the spectra (de-noising), minimizes the insignificant spectral

perturbations (smoothing) and decreases the size of the data matrix (compression). Fig. 2C shows good clustering for the first three principal components obtained by applying the PCA on the sparse matrix of thresholded wavelet coefficients. In this case spectra 42 and 28 appear on the edge of the cluster around the reference.

For a quantitative analysis of the three schemes we have evaluated a compression factor, a de-noising factor, a clustering factor and the CPU time for the PCA (Table 1). Compression, de-noising and clustering factors are better for scheme B compared to scheme A owing to the reduced noise in spectra. For scheme C the de-noising factor is better than for schemes A and B owing to the larger number of zeroes in the thresholded matrix.

Table 1  
Compression factors, de-noising factors, clustering factors, and elapsed CPU time<sup>a</sup>

Scheme	Compression factor	De-noising factor	Clustering factor	CPU time <sup>a</sup> (s)
A	1008	0.858	0.106	0.58
B	1231	0.861	0.198	0.41
C	11	0.903	0.346	15.25

<sup>a</sup> CPU time required for the principal component analysis of the pre-processed data.

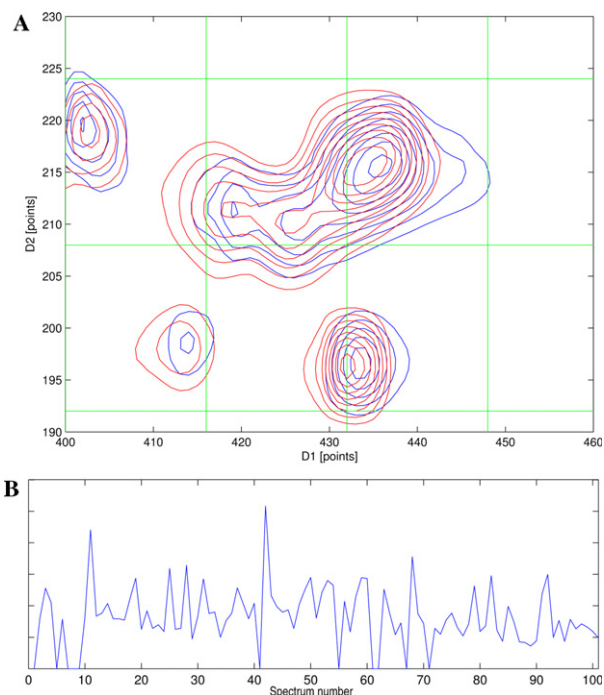


Fig. 3. (A) Example of peaks which cause a border effect in the bucketing schemes. Blue corresponds to spectrum 42 and red to the reference. The green grid represents the bucket borders. (B) Summed squared differences between each of the 101 spectra and the reference spectrum calculated at the bucket borders. For a better visualization all the spectra identified as true hits were excluded from this analysis (zeroes in the plot). (For interpretation of the references to color in this figure legend, the reader is referred to the web version of this paper.)

However, the compression factor is lower because the number of common zeroes between all spectra is much lower for de-noising in wavelet space than for de-noising of the actual spectra. The separation of outliers from the cluster representing spectra of protein with non-binding ligands is greatly improved in scheme C. This leads to a higher clustering factor compared to schemes A and B. The lower compression rate of scheme C leads to increased CPU time.

Further analysis of the false hit 42 in the bucketing schemes showed that it is not the outcome of the local noise dissimilarities but rather a consequence of the artifacts resulting from peak shifts in the vicinity of the bucket borders. Fig. 3A shows an example of signals in spectrum 42 which cause border artifacts in bucketing. When several effects of this kind are accumulated in one spectrum relatively large principal components will be observed. This cumulative effect can be shown by computing the sum of the squared differences between the reference and each spectrum at bucket borders. Fig. 3B shows that this function has a clear maximum for spectrum 42 due to an accumulation of bucket border artifacts. The effect of artifacts on bucket borders has also been confirmed using simulated spectra (not shown).

## 5. Discussion

While PCA has become a standard technique for data reduction and visualization of large data sets, the preparation of NMR data for PCA remains difficult. Filters applied prior to PCA should reduce the size of data to improve computational efficiency and minimize the sensitivity towards small irrelevant shifts in the NMR data. This has typically been achieved employing bucketing as a simple and highly efficient filter. Unfortunately bucketing may introduce artifacts when peaks move on borders between buckets and in the case of spectra with large variations of the background noise levels. The addition of spectral points into one bucket causes a modest reduction of noise depending on the size of the bucket. However, large buckets would be required to achieve a noticeable noise reduction. Applying a threshold to the experimental data is a frequently used alternative. Nevertheless, sharp thresholds tend to distort the buckets leading to more severe artifacts. In addition, with increasing resolution of spectra at higher magnetic fields with proton frequencies of up to 900 MHz, typical bucketing schemes reduce the effective resolution substantially. For this reason more subtle methods of smoothing and noise suppression are required.

In this work it has been shown that wavelet de-noising is a suitable alternative with desirable properties for subsequent PCA analysis. Here we have tested several schemes which combine the wavelet transforms to sup-

press noise-related coefficients with the PCA analysis. When PCA was applied to spectra after wavelet de-noising subsequent bucketing was still required to reduce the size of the data (scheme B). This scheme showed improved clustering owing to the reduced noise contribution to buckets. It also eliminates the noise-related artifacts observed for spectrum 28, but not the bucketing artifacts observed for spectrum 42.

Further improved clustering was achieved when PCA was directly applied to the wavelet coefficients (scheme C). This scheme eliminates noise-related (spectrum 28) and bucketing artifacts (spectrum 42) efficiently. The scheme offers a modest and scalable smoothing for one- or two-dimensional NMR data. The result can be optimized by selecting threshold levels in wavelet space and suitable levels to be suppressed in MRA. The effect of MRA will become more pronounced for data sets with baseline distortions typical for one-dimensional spectra.

Although the formation of data buckets is computationally less demanding than calculating the wavelet transformation, the additional computational effort seems justified considering the preservation in fine structure and the reduction in artifacts that can be achieved. The computing time of the lifting scheme used to obtain the wavelet coefficients [23] is proportional to the number of data points  $N$  of the data set and therefore by a factor of  $\log(N)$  faster than the fast Fourier transformation. In scheme C where PCA is performed in wavelet space no inverse transform is required. Once data are represented in wavelet space different thresholding or MRA schemes can be applied rapidly.

In conclusion, we propose a novel algorithm for the analysis of NMR screening data which combines the advantages of wavelet data representation with data visualization and clustering obtained by PCA. Using PCA and MRA in wavelet space we were able to obtain improved clustering and to avoid noise- and clustering-related artifacts. This approach should be commonly useful for many applications employing PCA in chemometrics.

## Acknowledgments

This work was supported by the European Large Scale Facility in Frankfurt, Germany. We thank D. Jacobs for kindly providing HSQC spectra of hsp90.

## References

- [1] B. Stockmann, C. Dalvit, NMR screening techniques in drug discovery and drug design, *Progr. Nucl. Magn. Spectrosc.* 41 (2002) 187–231.
- [2] S. Shuker, P. Hajduk, R. Meadows, S. Fesik, Discovering high-affinity ligands for proteins: SAR by NMR, *Science* 274 (1996) 1531–1534.
- [3] B. Meyer, T. Weimar, T. Peters, Screening mixtures for biological activity by NMR, *Eur. J. Biochem.* 246 (3) (1997) 705–709.
- [4] M. Vogtherr, P. Peters, Application of NMR based binding assays to identify key hydroxy groups for intermolecular recognition, *J. Am. Chem. Soc.* 122 (2000) 6093–6099.
- [5] M. Mayer, B. Meyer, Group epitope mapping by saturation transfer difference NMR to identify segments of a ligand in direct contact with a protein receptor, *J. Am. Chem. Soc.* 123 (25) (2001) 6108–6117.
- [6] M. Mayer, B. Meyer, Characterization of ligand binding by saturation transfer difference NMR spectra, *Angew. Chem. Int. Ed.* 35 (1999) 1784–1788.
- [7] M. Mayer, B. Meyer, Mapping the active site of angiotensin-converting enzyme by transferred NOE spectroscopy, *J. Med. Chem.* 43 (11) (2000) 2093–2099.
- [8] I. Bertini, C. Dalvit, J. Huber, C. Luchinat, M. Piccioli, ePHOGSY experiments on a paramagnetic protein: location of the catalytic water molecule in the heme crevice of the oxidized form of horse heart cytochrome *c*, *FEBS Lett.* 415 (1) (1997) 45–48.
- [9] M. Lin, M.J. Shapiro, J.R. Wareing, Diffusion-edited NMR-affinity NMR for direct observation of molecular interactions, *J. Am. Chem. Soc.* 119 (22) (1997) 5249–5250.
- [10] A. Chen, M.J. Shapiro, NOE pumping. 2. A high-throughput method to determine compounds with binding affinity to macromolecules by NMR, *J. Am. Chem. Soc.* 122 (2) (2000) 414–415.
- [11] A. Chen, M.J. Shapiro, NOE pumping: A novel NMR technique for identification of compounds with binding affinity to macromolecules, *J. Am. Chem. Soc.* 120 (39) (1998) 10258–10259.
- [12] J. Lindon, J. Nicholson, E. Holmes, J. Everett, Metabonomics: metabolic process studied by NMR spectroscopy of biofluids, *Concepts Magn. Reson.* 12 (5) (2000) 289–320.
- [13] J. Nicholson, J. Connelly, J. Lindon, E. Holmes, Metabonomics: a platform for studying drug toxicity and gene function, *Nat. Rev. Drug. Discov.* 1 (2) (2002) 153–161.
- [14] P. Belton, I. Colquhoun, E. Kemsley, I. Delgadillo, P. Roma, M. Dennis, M. Sharman, E. Holmes, J. Nicholson, M. Spraul, Application of chemometrics to the  $^1\text{H}$  NMR spectra of apple juices: discrimination between apple varieties, *Food Chem.* 61 (1998) 207–213.
- [15] J. Vercauteren, D. Rutledge, Multivariate statistical analysis of 2D NMR data to differentiate grapevine cultivars and clones, *Food Chem.* 57 (1996) 441–450.
- [16] I. Duarte, A. Barros, P. Belton, R. Righelato, M. Spraul, E. Humpfer, A. Gil, High-resolution nuclear magnetic resonance spectroscopy and multivariate analysis for the characterization of beer, *J. Agric. Food Chem.* 50 (9) (2002) 2475–2481.
- [17] A. Ross, G. Schlotterbeck, W. Klaus, H. Senn, Automation of NMR measurements and data evaluation for systematically screening interactions of small molecules with target proteins, *J. Biomol. NMR* 16 (2) (2000) 139–146.
- [18] J. Buckheit, D. Donoho, Wavelab and reproducible research, in: A. Antoniadis, G. Oppenheim (Eds.), *Wavelets and Statistics*, Springer, Berlin, 1995, pp. 53–81.
- [19] J.C. Hoch, A.S. Stern, *NMR Data Processing*, Wiley-Liss, New York, 1996.
- [20] H.F. Cancino-De-Greiff, R. Ramos-Garcia, J.V. Lorenzo-Ginori, Signal de-noising in magnetic resonance spectroscopy using wavelet transforms, *Concepts Magn. Reson.* 14 (6) (2002) 388–401.
- [21] X.-G. Shao, A. Kai-Man Leung, F.-T. Chau, Wavelet: a new trend in chemistry, *Ace. Chem. Res.* 36 (2003) 276–283.
- [22] I. Daubechies, *Ten Lectures on Wavelets*, SIAM, Philadelphia, 1992.
- [23] S. Mallat, *A Wavelet Tour of Signal Processing*, Academic Press, 1998.
- [24] D. Donoho, I. Johnstone, Ideal spacial adaptation via wavelet shrinkage, *Biometrika* 81 (1994) 425–455.
- [25] D. Donoho, I. Johnstone, Adapting to unknown smoothness via wavelet shrinkage, *J. Am. Stat. Assoc.* 90 (1995) 1200–1224.

- [26] S. Mallat, Multiresolution approximations and wavelet orthonormal bases of  $L^2(\mathbb{R})$ , *Trans. Am. Math. Soc.* 315 (1989) 69–87.
- [27] U. Günther, C. Ludwig, H. Rüterjans, Wavelet-improved solvent suppression in NMR spectra employing wavelet transforms, *J. Magn. Reson.* (2002) 19–25.
- [28] U. Gunther, C. Ludwig, H. Rüterjans, NMRLAB-advanced NMR data processing in matlab, *J. Magn. Reson.* 145 (2) (2000) 201–208.
- [29] S.C. Johnson, Hierarchical clustering schemes, *Psychometrika* 2 (1967) 241–254.